

## Viscous mechanism for Leidenfrost propulsion on a ratchet

G. DUPEUX<sup>1,2</sup>, M. LE MERRER<sup>1,2</sup>, G. LAGUBEAU<sup>1,2</sup>, C. CLANET<sup>1,2</sup>, S. HARDT<sup>3</sup> and D. QUÉRÉ<sup>1,2(a)</sup>

<sup>1</sup> *Physique et Mécanique des Milieux Hétérogènes, UMR 7636 du CNRS, ESPCI - 75005 Paris, France, EU*

<sup>2</sup> *Ladhyx, UMR 7646 du CNRS, École Polytechnique - 91128 Palaiseau Cedex, France, EU*

<sup>3</sup> *Center for Smart Interfaces, Technische Universität Darmstadt - Petersenstraße 32, D-64287 Darmstadt, Germany, EU*

received 3 August 2011; accepted in final form 7 October 2011

published online 22 November 2011

PACS 83.50.Lh – Slip boundary effects (interfacial and free surface flows)

**Abstract** – An evaporating drop placed on a ratchet self-propels, as discovered by Linke *et al.* in 2006. Sublimating platelets do the same, and we discuss here a possible viscous mechanism for these motions. We report that the flow of vapor below the levitating material is rectified by the asymmetric teeth of the ratchet, in the direction of descending slopes along each tooth. As a consequence, the resulting viscous stress can entrain the material in the same direction, and we discuss the resulting self-propelling force.

editor's choice Copyright © EPLA, 2011

Non-wetting liquid states recently attracted a lot of attention, owing to the extreme mobility of drops in such situations [1–3]. A liquid on a hot solid achieves pure non-wetting, since it levitates on a cushion of its own vapor (Leidenfrost effect). Even tiny forces are sufficient to displace it, instead of forces on the order of the drop weight, in usual cases [4]. Linke's device, discovered in 2006, is a spectacular illustration of this principle. Linke *et al.* considered hot ratchets on which drops were found to self-propel, and suggested that the motion originates from the viscous drag by the vapor flowing below the drop [5]. The corresponding forces  $F$  were measured and found to be typically  $10 \mu\text{N}$ , and to increase with the equatorial radius  $R$  of the drop, in the interval between 2 and 10 mm [5,6]. At these scales, drops are flattened by gravity, and can be viewed as disks of radius  $R$  and thickness twice the capillary length (2.5 mm for water at  $100^\circ\text{C}$ , 1 mm for liquid nitrogen) [7]. Teeth also generate a special friction, as the liquid hits their steps [6]. They were originally millimetric in size, but similar effects were also found on much smaller ratchets [8].

Ratchets also permit the propulsion of Leidenfrost solids: platelets of dry ice (solid carbon dioxide that directly sublimates at atmospheric pressure) placed on hot ratchets self-propel in the same direction as drops, as indicated in fig. 1(b) [6]. This experiment clearly shows that the motion originates from the production of vapor below the levitating body, and not necessarily to its liquid (*i.e.* deformable) nature. Once the vapor is produced, it

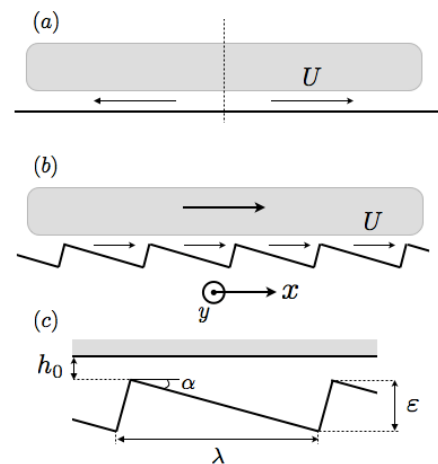


Fig. 1: A platelet of dry ice (centimetric radius, millimetric height, sublimation temperature of  $-80^\circ\text{C}$ ) is placed above a hot substrate (temperature of  $450^\circ\text{C}$ ). The platelet levitates (Leidenfrost phenomenon), and we discuss the flow of vapor in the thin layer separating the platelet from the substrate. The substrate is either flat (a), or consists of a ratchet, which propels the dry ice in the direction indicated by the bold arrow (b). We denote  $U$  as the typical velocity of the vapor flow (assumed here to be anisotropic). (c) Definition for the different lengths of the system.

flows between the platelet and the substrate. This flow is expected to be isotropic on a flat solid (fig. 1(a)), where it does not produce a directional force. But a ratchet may rectify the flow of vapor (as suggested in fig. 1(b)), which

<sup>(a)</sup>E-mail: david.quere@espci.fr

can induce a propelling force on the levitating object. Yet several possibilities remain for explaining the motion:

- i) At high Reynolds numbers, inertial effects induce a rectification of the vapor flow, but the direction of the flow is not clearly established. Thiria and Zhang recently showed that oscillating a flat plate above a ratchet immersed in water can rectify the flow in the direction of negative  $x$ , provided the Reynolds number is a few hundreds [9]. But it has also been shown in channels with converging or diverging walls that flow resistance can be higher in this direction [10,11], which favors a flow in the opposite direction. This effect was exploited in nozzle-diffuser micropumps incorporating valves without moving parts.
- ii) At moderate Reynolds numbers, rectification may also occur in the direction of positive  $x$ , as the lubricating vapor flows along the descending steps of the ratchet. However, there is today no direct proof of that, and this paper aims at showing the existence of such a directional flow.

Whatever the direction of the vapor flow, two effects can produce a force on the levitating platelet (or drop). On the one hand, a directional ejection of vapor can generate a rocket effect, propelling the object in the direction opposite to the flow, as proposed in [6]. On the other hand, a viscous stress drags the platelet in the direction of the gas flow, as sketched in fig. 1(b) [5]. In order to clarify the origin of the motion, we need to perform a local analysis of the vapor flow. In this paper, we wonder whether the ratchet rectifies the flow, and if yes, in which direction relative to the motion of the droplet/platelet. Answers to these questions should allow us to discriminate between the different scenarii for the motion.

In our experiment, we make platelets from small pellets of dry ice (radius  $R = 0.65$  cm). We sublime the pellet on a hot flat plate to control its thickness  $H$  between 1 mm and 1 cm. The resulting disk is held by a wood clip attached to a microscrew, allowing us to bring it close to a hot metallic solid ( $T = 450$  °C), which is either flat or covered by a ratchet (tooth length  $\lambda = 1.5$  mm, tooth height  $\varepsilon = 250$   $\mu\text{m}$ , which gives textures tilted by  $\alpha = 10^\circ$  to the horizontal, as defined in fig. 1(c)). We sprinkle on the solid glass beads (radius  $r = 25$   $\mu\text{m}$ , and density  $\rho_S = 2500$  kg/m<sup>3</sup>), and observe the thin vapor layer between the dry ice and the solid. Contrast is obtained with backlighting, and movies are shot at typically 1000 frames per second with an Optronics CamRecord, mounted with a macro objective of 50 mm. The field depth is 2 mm, and the focus is made in the vertical plane, 5 mm further than the front of the disk of ice.

Typical movies ([Dry-ice-on-flat-plate.avi](#) and [Dry-ice-on-ratchet.avi](#)) are shown online (see the supplementary information in footnote <sup>1</sup>), and fig. 2

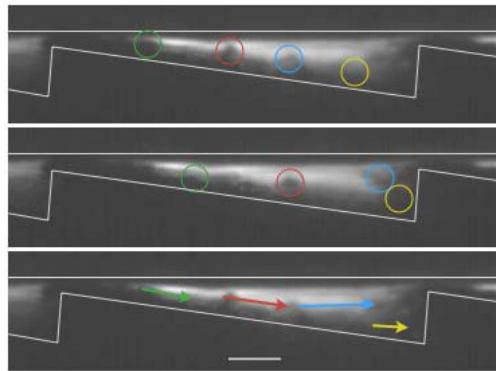


Fig. 2: (Color online) Vapor flow at the scale of one tooth of length  $\lambda = 1.5$  mm and height  $250$   $\mu\text{m}$ . Glass beads are first deposited on the ratchet, and four of them are followed as a piece of dry ice is brought close to the ratchet (the bottom of the ice is underlined by a thin horizontal line, ratchet temperature  $450$  °C). 3 ms separate the two first images, from which we can deduce the average velocity of the vapor flow in this time interval (third image). The vapor velocity is directed towards the tooth step, and its intensity is on the order of  $10$  cm/s. The bar at the bottom represents  $200$   $\mu\text{m}$ . See the supplementary information for the corresponding movie in footnote <sup>1</sup>.

shows how they can be analyzed. We present a zoom on a single tooth, underlined by a thin white line. The bottom of the disk of dry ice is indicated by a horizontal line (the minimum distance between the ice and the teeth is  $60$   $\mu\text{m}$ , comparable to the distance observed on self-propelling platelets). We can follow the displacement of four different beads between the first and second image, which are separated by 3 ms. For clarity, each bead is surrounded by a colored circle. It is observed that the vapor flow entrains the beads, from which we deduce an average flow velocity shown in the third image by colored arrows. The bar represents  $200$   $\mu\text{m}$ , so that we find (from right to left) velocities in the  $x$ -direction of 8, 11, 14 and 5 cm/s. We also see on the picture the clouds resulting from the condensation of water present in air, close to dry ice.

Figure 2 and the corresponding movies unambiguously show that the vapor flow in this experiment is anisotropic, and directed along the descending slope of the teeth (*i.e.* toward positive  $x$  in fig. 1(b)). The beads first accelerate, and the characteristic time  $\tau$  for reaching the vapor velocity is obtained by balancing the bead inertia with the viscous drag of vapor (of viscosity  $\eta$ ), which yields  $\tau = 2\rho_S r^2 / 9\eta$ . Hence  $\tau$  is approximately 10 ms, comparable to the traveling time  $\lambda/U$  of vapor along a tooth: bead velocities hardly underestimate the mean vapor flow velocity, and will thus be taken as tracers of this flow. By following 100 such tracers, we could eventually

close to them. In the first movie, [Dry-ice-on-flat-plate.avi](#), the substrate is flat (corresponding to figs. 1(a) and 3(a)); in the second one, [Dry-ice-on-ratchet.avi](#), it consists of a ratchet (corresponding to figs. 1(b), 2 and 3(b)).

<sup>1</sup>Two movies showing how microbeads first placed on hot substrates ( $T = 450$  °C) move as platelets of dry ice are approached

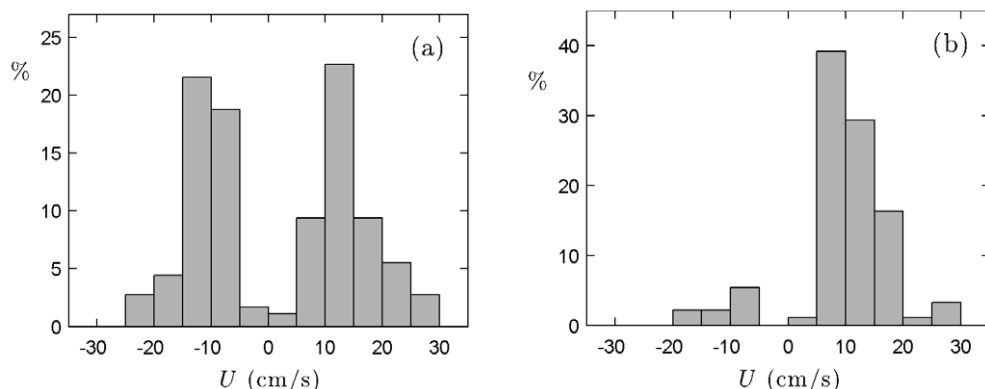


Fig. 3: Histograms of the vapor flow velocity below a Leidenfrost platelet of dry ice. The average velocity of the flow is deduced from tracers as shown in fig. 2, and the percentage of beads having a given velocity is plotted as a function of the velocity. Positive velocities are directed in the direction of positive  $x$  (as defined in fig. 1). (a) Vapor flow above a flat surface, as sketched in fig. 1(a). (b) Vapor flow above the ratchet shown in fig. 2. The latter histogram confirms the ability of ratchets to rectify the vapor flow. Both substrates are heated to a temperature of  $450^\circ\text{C}$ . See the supplementary information for the corresponding movies in footnote <sup>1</sup>.

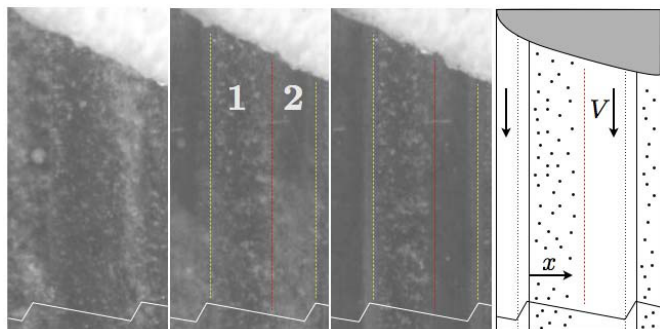


Fig. 4: (Color online) Top view of the experiment. The ratchet is first covered by microbeads (first image), and dry ice is approached (white, at the top in the photos). The vapor flow below the ice is evacuated along the teeth steps, as revealed by the cloudy zone along each step (underlined by a yellow line). Slightly later (third image), the microbeads have been swept by the vapor close to the step (zone 2), while the lateral vapor flow is too weak to entrain them far from the step (zone 1).

build histograms of the average velocity of the vapor flow, as shown in fig. 3, where we compare vapor velocity above a flat substrate and above a ratchet, both at a temperature of  $450^\circ\text{C}$ .

The tracer velocity is observed in both cases to be on the order of  $10\text{ cm/s}$ . The flow is isotropic above a flat plate (fig. 3(a)), but it clearly becomes anisotropic above a ratchet (fig. 3(b)): a direct measurement confirms the ability of ratchets to rectify the vapor flow, and show that this flow mainly takes place, for this series of experiment, in the direction assumed in fig. 1(b). Results comparable to the observations in figs. 2 and 3(b) were obtained by looking below self-moving platelets placed on hot ratchets.

It is also useful to understand how the vapor flow is affected as it hits the teeth steps. The few data in fig. 3(b) with negative velocities correspond to beads that bounced

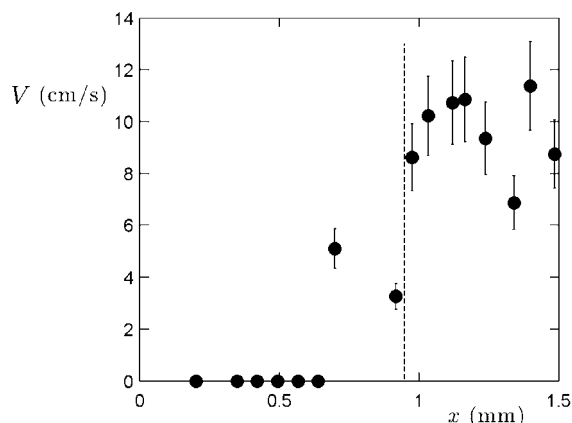


Fig. 5: Vapor flow perpendicular to the platelet motion: the flow escaping along each tooth step is characterized by a velocity  $V$  on the order of  $10\text{ cm/s}$ , and it remains localized along the step (zone 2 in fig. 4): there is no appreciable vapor flow at a distance from the step ( $x = \lambda = 1.5\text{ mm}$ ) larger than  $0.5\text{ mm}$ , *i.e.* one-third of the tooth width  $\lambda$ .

off the step, but the flow seems clearly different from rolls in the teeth (which would generate an equal amount of positive and negative velocities). A movie taken from above helps to clarify the behavior of the gas in this region, and we show in figs. 4, 5 and 6 the results of this investigation.

In the first image of fig. 4, the dry ice (right top corner, in white) is still far from the surface, and we can distinguish the layer of microbeads placed on the ratchet. In the second image, the beads remain at rest in the higher part of the tooth (zone 1), while a blurred band (zone 2) is observed close to the tooth step, which reveals a lateral flow in this region: as it hits the step, the vapor flees along the direction  $y$  defined in fig. 1(b), and sweeps the microbeads. Slightly later (third image), black bands are visible along each step, corresponding to

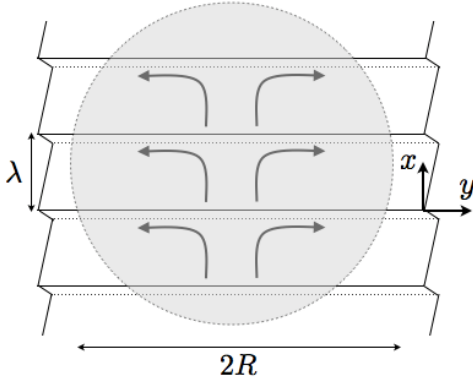


Fig. 6: The vapor flow between the ratchet and the dry ice (in grey) is cellular: each tooth carries a flow in the direction of positive  $x$ , which gets evacuated along the step.

a complete sweeping of the particles in zone 2 due to this escaping flow, as sketched in the fourth image. This flow is symmetric in the direction of positive and negative  $y$ , so that it does not exert a net force on the platelet. We denote  $V$  the characteristic velocity of this flow in the  $y$ -direction, orthogonal to  $U$ .

By analyzing the motion of the beads a few millimeters aside from dry ice, we can build the profile of this lateral flow along the step, taking it as the origin in  $x$ , and focusing on one tooth, of length  $\lambda = 1.5$  mm. We report in fig. 5 this velocity profile. It is observed that the orthogonal flow velocity  $V$  is again on the order of 10 cm/s ( $V \approx U$ ), and that the flow remains localized in the vicinity of the step —at a distance larger than  $\lambda/3$ , we do not record any appreciable motion of vapor.

On the whole, our experimental findings show that flow rectification does occur on the ratchet, in the direction of the descending slope of the teeth. When the vapor flow hits the next step, it gets deflected by ninety degrees and evacuated along the step. This implies that the flow below a piece of dry ice is cellular: each tooth develops a similar and independent flow, as sketched in fig. 6, so that the total force acting on the ice is the sum of  $N = 2R/\lambda$  individual contributions.

We can be more precise about a scenario of propulsion. The Reynolds number  $Re$  of the vapor flow is obtained by comparing inertia (of order  $\rho U^2/\lambda$ ) with viscous resistance (of order  $\eta U/h^2$ , where  $\rho$  is the vapor density and  $h$  the typical thickness of the vapor film). The resulting Reynolds number  $Re = \rho U h^2/\eta \lambda$  can be estimated from our experiments. We have  $U \approx 10$  cm/s (taking the tracer velocity as characteristic of the flow),  $h \approx 100$   $\mu$ m (since the levitation height  $h_o$  is 50  $\mu$ m, and the teeth height  $\varepsilon$  is 250  $\mu$ m),  $\rho \approx 1$  kg/m<sup>3</sup>, and  $\eta \approx 3 \cdot 10^{-5}$  Pa.s. (Gas viscosity increases as the square root of temperature. The mean temperature between the hot substrate and the platelet is 270 °C, a temperature at which the gas viscosity is typically 30 to 40% higher than at room temperature.) Hence the Reynolds number is expected to be of order 0.1. Together with the observations in figs. 2 and 3(b), this

strongly suggests that Leidenfrost platelets on a ratchet are entrained by the viscous stress generated by the vapor flow. Denoting  $h$  as the mean thickness of vapor, we then expect a force per tooth

$$f \sim \frac{\eta U}{h} R \lambda. \quad (1)$$

The gas velocity  $U$  should be given by the Poiseuille law, and thus scale as  $(h^2/\eta)(dP/dx)$ . The pressure gradient  $dP/dx$  driving the gas flow arises from the platelet weight  $Mg$ , which generates a pressure  $Mg/R^2$ , and a pressure gradient scaling as  $Mg/R^2\lambda$ . Once we multiply the resulting force by the number of cells  $R/\lambda$  below the ratchet, we find a driving force scaling as  $Mgh/\lambda$ . In a first approximation ( $h_o \ll \varepsilon$ , where the different dimensions are defined in fig. 1(c)),  $h/\lambda$  is taken as  $\alpha$ , the angle by which the teeth are inclined to the horizontal ( $\alpha = 10^\circ$  in our experiment). Hence we get for the total force driving the platelet:

$$F \sim Mg\alpha. \quad (2)$$

Logically, this force is an odd function of  $\alpha$  (if  $\alpha$  becomes  $-\alpha$ , motion takes place in the opposite direction), and it vanishes with this ratchet parameter. Since the Poiseuille law between two solid plates implies a numerical factor 1/12, we expect  $F$  to be on the order of 10 to 100  $\mu$ N, as observed experimentally [5,6].  $F$  is also a function of the platelet weight  $\rho_o g H R^2$  (with  $\rho_o \approx 1500$  kg/m<sup>3</sup> for dry ice), since the weight causes the gas flow responsible for the motion. The force increase as  $R^2$  is close to the observations reported in [6].

The way the force varies with the ice height  $H$  can be also tested: since our levitating body is solid, it is possible to vary its height independently of its radius. We performed a series of experiments on self-propelling platelets, for  $H$  between 0.75 and 9 mm. The platelet is thrown in the direction of negative  $x$ , so that it slows down, stops and accelerates in the direction of positive  $x$ . The trajectory  $x(t)$  is fitted around the arrest point on 2 cm with a parabola, from which we deduce the platelet acceleration  $a$ , and the force  $F = Ma$  propelling it. The duration of an experiment is typically 1 s, much smaller than the sublimation time of the platelet (of order 1 min.), so that  $M$  can be considered as constant during the experiment. We plot in fig. 7 the force  $F$  as a function of the platelet thickness  $H$ , and observe that the force indeed increase with  $H$ , in a fashion compatible with a linear law (the solid line has a slope 1), as expected from eq. (2). Note that this first naive attempt might be improved by taking into account the lateral escaping flow.

Ratchet-like materials generate special dynamical properties: they are known to induce anisotropic friction or adhesion [12,13], and self-propulsion in a Leidenfrost situation [5,6]. Here we showed that the motion of Leidenfrost platelets on ratchets can be explained by the viscous stress generated by the rectified flow of vapor. This flow starts at the teeth tops, flows down the teeth, and gets

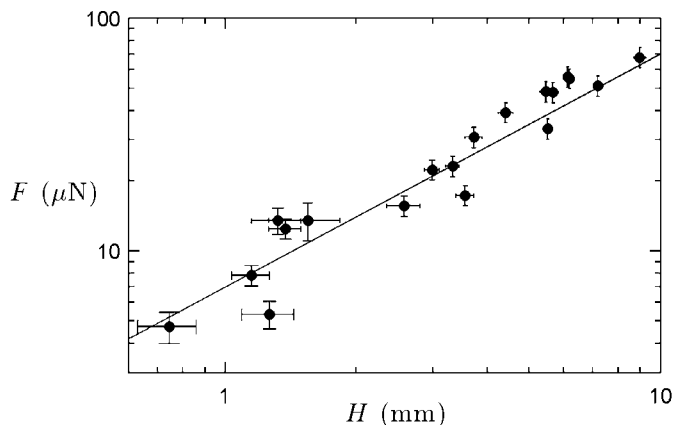


Fig. 7: Force acting on a platelet of dry ice ( $R = 0.65$  mm) placed on a hot ratchet ( $T = 450$  °C, teeth length  $\lambda = 1.5$  mm, teeth height  $250$   $\mu$ m).  $F$  is deduced from the platelet acceleration. The data are obtained for various platelet thicknesses  $H$ , between  $0.75$  and  $9$  mm. Slope 1 is shown with a solid line, and found to be in good agreement with the data, as expected from eq. (2).

evacuated along the steps. The direction of the vapor flow is crucial to distinguish between inertial and viscous propulsion. Together with the observed moderate values of the Reynolds number, our findings show that the viscous mechanism should be dominant, confirming a scenario proposed by Linke *et al.* for explaining drop propulsion on hot ratchets [5]. We were recently informed that Cousins *et al.* reached the same conclusion, for systems made of concentric teeth [14]. This result contrasts with a previous model we made, where the Reynolds number was overestimated, leading to an inertial propelling force [6]. The three-dimensional character of the flow matters, since it makes the flow cellular at the tooth scale: each tooth produces an independent drag, and their sum defines the entrainment force. More complicated ratchet designs (such as zig-zag teeth) should thus affect the motion—a stimulating topic for future research in the field. It would also be of interest to check whether these findings also hold for drop motion, for which the deformable nature of the interfaces might affect the vapor flow characteristics.

\*\*\*

We thank RAY GOLDSTEIN, HEINER LINKE, BENJAMIN THIRIA and JUN ZHANG for fruitful discussions.

#### APPENDIX

We discuss here in more detail the scaling law for the force driving the platelet. As sketched in fig. 6, the complex geometry of the system creates a 3D flow, so that the exact lubrication calculation cannot be solved analytically. However, we can find an expression for the driving force by writing the motion equations in the lubrication approximation, and discuss how the resulting lift and drag forces depend on the ratchet angle  $\alpha$ . Firstly,

the mean gas velocity at position  $x$  is given by the Poiseuille law:  $U \sim (h^2/\eta)(dP/dx)$ , where  $h = h_o + \alpha x$  is the distance between the platelet and the ratchet surface (fig. 1(c)). Secondly, the local flux conservation can be written:  $d(hUR)/dx \sim (\kappa R \Delta T / \rho L h)$ , where we classically assumed that conduction dominates the heat transfer, and denoted  $\Delta T$  as the temperature difference between the solid and the platelet,  $\kappa$  as the thermal conductivity of the vapor, and  $L$  as the latent heat of sublimation [15]. We deduce from these equations that the pressure scales as  $P_o \sim \lambda^2 \eta \kappa \Delta T / \rho L h_o^4$ . We can now calculate the normal force and tangential (driving) force generated by the vapor motion. On the one hand, the normal force is

$$F_N \sim \frac{R}{\lambda} R \int_0^\lambda P(x) dx \sim \frac{R^2 \lambda^2 \eta \kappa \Delta T}{\rho L h_o^4} \int_0^1 P^*(x^*) dx^* \sim P_o R^2 f(\alpha^*), \quad (\text{A.1})$$

where the stars indicate dimensionless quantities ( $P^* = P/P_o$ ,  $x^* = x/\lambda$  and  $\alpha^* = \alpha\lambda/h_o$ ).  $F_N$  is balanced by the platelet weight  $Mg$  to satisfy levitation, so that its expression should work both for  $\alpha = 0$ , and for  $\alpha \neq 0$ . Hence we expect the function  $f$  to be a constant. Balancing the normal force  $F_N \sim P_o R^2$  with the platelet weigh yields a scaling law for the thickness  $h_o$  [7].

On the other hand, the tangential drag force is

$$F_T \sim \frac{R}{\lambda} R \int_0^\lambda \eta \left. \frac{\partial u}{\partial y} \right|_h dx \sim \frac{R^2 \lambda \eta \kappa \Delta T}{\rho L h_o^3} \int_0^1 h^* \frac{dP^*}{dx^*} dx^* \sim \frac{R^2 \lambda \eta \kappa \Delta T}{\rho L h_o^3} g(\alpha^*). \quad (\text{A.2})$$

The function  $g$  must vanish for  $\alpha^* = 0$ , and it must be an odd function of  $\alpha^*$ , for symmetry reason. Hence we expect  $g$  to be at first order linear in  $\alpha^*$ , which, once we use eq. (A.1) and the balance  $F_N \sim Mg$ , brings us back to eq. (2).

#### REFERENCES

- [1] MAHADEVAN L. and POMEAU Y., *Phys. Fluids*, **11** (1999) 2449.
- [2] YOSHIMITSU Z., NAKAJIMA A., WATANABE T. and HASHIMOTO K., *Langmuir*, **18** (2002) 5818.
- [3] REYSSAT M., RICHARD D., CLANET C. and QUÉRÉ D., *Faraday Discuss.*, **146** (2010) 19.
- [4] PODGORSKI T., FLESSELLES J. M. and LIMAT L., *Phys. Rev. Lett.*, **87** (2001) 036102.
- [5] LINKE H. *et al.*, *Phys. Rev. Lett.*, **96** (2006) 154502.
- [6] LAGUBEAU G., LE MERRER M., CLANET C. and QUÉRÉ D., *Nat. Phys.*, **7** (2011) 395.
- [7] BIANCE A. L., CLANET C. and QUÉRÉ D., *Phys. Fluids*, **15** (2003) 1632.
- [8] OK J. T., LOPEZ-ONNA E., NIKITPOULOS D. E., WONG H. and PARK S., *Microfluid. Nanofluid.*, **10** (2011) 1045.
- [9] THIRIA B. and ZHANG J., private communication (2011).

- [10] JIANG X. N., ZHOU Z. Y., HUANG X. Y., LI Y., YANG Y. and LIU C. Y., *Sens. Actuators A*, **70** (1998) 81.
- [11] YANG K. S., CHEN I. Y., SHEW B. Y. and WANG C. C., *J. Micromech. Microeng.*, **14** (2004) 26.
- [12] ZHENG Y., GAO X. and JIANG L., *Soft Matter*, **3** (2007) 178.
- [13] MALVADKAR N. A., HANCOCK M. J., SEKEROGLU K., DRESSICK W. J. and DEMIREL M. C., *Nat. Mater.*, **9** (2010) 1023.
- [14] COUSINS T. R., GOLDSTEIN R. E., JAWORSKI J. W. and PESCI A. I., to be published in *J. Fluid Mech.* (2011).
- [15] GOTTFRIED B. S., LEE C. J. and BELL K. J., *Int. J. Heat Mass Transfer*, **9** (1966) 1167.